

Geophysical Research Letters®

RESEARCH LETTER

10.1029/2023GL106863

The Response of Surface Temperature Persistence to Arctic Sea-Ice Loss

Neil T. Lewis¹ , William J. M. Seviour^{1,2}, Hannah E. Roberts-Straw³, and James A. Screen¹ 

¹Department of Mathematics and Statistics, University of Exeter, Exeter, UK, ²Global Systems Institute, University of Exeter, Exeter, UK, ³Natural Sciences, University of Exeter, Exeter, UK

Key Points:

- Arctic sea-ice loss drives local increases in persistence by reducing the effective heat capacity of the surface
- Persistence in midlatitudes increases due to changes in the forcing of surface temperature variability by atmospheric circulation
- The effect of sea-ice loss on persistence may be underestimated in comprehensive models with constrained sea-ice

Supporting Information:

Supporting Information may be found in the online version of this article.

Correspondence to:

N. T. Lewis,
n.t.lewis@exeter.ac.uk

Citation:

Lewis, N. T., Seviour, W. J. M., Roberts-Straw, H. E., & Screen, J. A. (2024). The response of surface temperature persistence to Arctic sea-ice loss. *Geophysical Research Letters*, *51*, e2023GL106863. <https://doi.org/10.1029/2023GL106863>

Received 18 OCT 2023

Accepted 19 JAN 2024

Abstract We investigate the response of surface temperature persistence, quantified using a lagged autocorrelation, to imposed Arctic sea-ice loss in coupled model experiments. Sea-ice loss causes increases in persistence over ocean in midlatitudes and the low-Arctic, which are of a similar magnitude to the total response to climate change in these regions. Using an idealized model, we show that sea-ice loss induces a slowing of meridional wind anomalies, which can drive the midlatitude persistence increase obtained in coupled models. Sea-ice loss should induce persistence increases in the Arctic, through its effect on the surface heat capacity. However, in coupled models with imposed sea-ice loss, persistence increase in the Arctic is essentially absent. We suggest that methods used to constrain sea-ice in coupled models may spuriously reduce the effects of sea-ice loss on persistence.

Plain Language Summary It has been suggested that Arctic sea-ice loss is driving an increase in extreme weather events in Northern Hemisphere midlatitudes. We discuss two routes through which Arctic sea-ice loss can increase the persistence of weather in the Arctic and midlatitudes. First, sea-ice loss increases the thermal inertia of the surface by exposing open ocean, which has a higher heat capacity, potentially leading to persistence increases in the Arctic. Second, sea-ice loss drives changes in atmospheric circulation, which may affect surface temperature variability. We analyze climate model experiments where sea-ice loss is artificially induced, in the absence of other climate forcings, to investigate whether either of these routes leads to an appreciable change in the persistence of surface weather. We find sea-ice loss causes modest increases in persistence in midlatitudes, with the most significant changes occurring over ocean regions. Unexpectedly, we do not identify an increase in Arctic persistence in these experiments, even though this response is easily identifiable in experiments driven by greenhouse gas emissions. Using a simplified climate model, we show that underestimating the persistence response may be an unintended side-effect of the methods used to isolate the effect of sea-ice loss in climate models.

1. Introduction

The Arctic is experiencing substantial sea-ice loss in response to global warming (Notz & Stroeve, 2016), which has contributed to enhanced near-surface warming at high-latitudes (Screen & Simmonds, 2010). High-latitude warming is expected to have an impact on the zonally-averaged circulation in the Northern Hemisphere, acting to weaken the jet and shift it equatorwards. This jet response has been identified in idealized (Butler et al., 2010) and comprehensive (Screen & Blackport, 2019; Smith et al., 2022) climate models, although there is a high degree of uncertainty in its magnitude, due to model spread in the strength of re-enforcing eddy-feedbacks (Smith et al., 2022).

It is plausible that changes in the jet stream will have an influence on the properties of midlatitude waves and storms, but the nature of any such effect, and whether or not it will have a discernible influence on surface weather, is still poorly understood (Barnes & Screen, 2015; Cohen et al., 2014, 2019). For example, Francis and Vavrus (2012) have argued that waves embedded on a weaker jet will propagate more slowly and undergo larger amplitude meanders, thus favoring more persistent weather. There has been little investigation of whether or not these (or other) changes in the circulation, induced by sea-ice loss, actually drive changes in the persistence of variables relevant to surface weather (e.g., surface temperature or precipitation).

A few studies have argued that climate change may drive increases in surface temperature persistence. Li and Thompson (2021) analyze changes in surface temperature persistence between the periods 1970–1999 and 2070–2099 in four large ensembles (LE) run under RCP8.5 forcing (Deser et al., 2020). In each LE, they find substantial

© 2024. The Authors.

This is an open access article under the terms of the [Creative Commons Attribution License](https://creativecommons.org/licenses/by/4.0/), which permits use, distribution and reproduction in any medium, provided the original work is properly cited.

increases in surface temperature persistence (measured using the autocorrelation of surface temperature), the largest of which occur in the Arctic and midlatitudes (with midlatitude change enhanced over ocean compared with land; see their Figure 3). Additionally, Pfleiderer and Coumou (2018) analyze observed daily temperature anomalies over land, and report an increase in persistence in midlatitudes during summer months over the second half of the 20th century. Li and Thompson (2021) emphasize the role of radiative feedbacks in driving persistence changes under climate change, while also noting the effect of Arctic sea-ice loss to increase persistence at high latitudes, through its effect on surface heat capacity. Less attention is given to the role of circulation changes, which may have an effect on persistence by altering the forcing spectrum of surface temperature variability.

The aim of this work is to investigate the role of sea-ice loss, and the associated response of atmospheric circulation, in driving changes in surface temperature persistence. We do this by analyzing output from coupled atmosphere-ocean general circulation model (AOGCM) simulations with constrained sea-ice, contributed to the Polar Amplification Inter-model Comparison Project (PAMIP; Smith et al., 2019). Our results are compared with those obtained from Historical/ScenarioMIP (ssp585) runs conducted using the same AOGCMs for which PAMIP output was available. Additionally, we make use of an idealized GCM to interpret the AOGCM results. Our methodology is described in Section 2, our results are presented in Section 3, and discussion is offered in Section 4.

2. Methods

2.1. AOGCM Output

To quantify the response of surface temperature persistence to Arctic sea-ice loss, we analyze near-surface air temperature from coupled AOGCM time-slice runs contributed to PAMIP (Smith et al., 2019). Two PAMIP experiments are used where Arctic sea-ice concentration (SIC) is nudged toward (a) “pre-industrial” SIC (pa-piArcSIC), and (b) “future” SIC (pa-futArcSIC). The target SICs are obtained from 30 year periods extracted from CMIP5 historical/RCP8.5 simulations where the time- and globally-averaged surface temperature is 13.67°C for pre-industrial SIC, and 15.67°C (i.e., 2°C warming) for future SIC. We use output from 4 models (number of ensemble members in brackets): HadGEM3-GC31-MM (300); IPSL-CM6A-LR (200); CESM2-WACCM (200); CESM1-WACCM-SC (100). We use output from coupled PAMIP experiments instead of the larger ensemble of atmosphere-only experiments as fixing sea surface temperature would damp the response of near-surface air temperature over ocean.

To compare the effect of Arctic sea-ice loss on persistence with the total change due to greenhouse gas forcing and climate change, we also analyze CMIP6 historical/ScenarioMIP (ssp585) runs (hereafter “CMIP6”). We use output from three of the models analyzed from PAMIP: HadGEM3-GC31-MM, IPSL-CM6A-LR, and CESM2-WACCM. For each model, three ensemble members are used. We identify 30 year pre-industrial and future periods as those where the time-averaged sea-ice area is equal to that in the equivalent PAMIP simulation. The time periods used for each CMIP6 model are specified in the Table S1 in Supporting Information S1. For the purposes of computing surface temperature persistence, each model year is analyzed separately in order to assess significance with respect to interannual variability. We note that comparing PAMIP time-slice, equilibrium runs with CMIP6 transient simulations does not make for a perfect one-to-one comparison (Kang et al., 2023; Sun et al., 2018). Previous work has shown that Arctic sea-ice loss only becomes important around the mid-21st century, so it is possible that the importance of sea-ice loss may be underrepresented in the 30 year future time periods we use for the CMIP6 models (which each terminate in the early or mid-21st century).

For both the PAMIP and CMIP6 output, all data is re-gridded onto a common 2.5° latitude-longitude grid prior to analysis. Computation of the autocorrelation utilizes data from the entire year, as opposed to isolating changes in a specific season (e.g., summer or winter), as we found that using short timeseries associated with individual seasons yielded statistically insignificant responses (for both CMIP6 and PAMIP).

2.2. Surface Temperature Persistence

Following Li and Thompson (2021), we quantify persistence at each grid point by computing the lagged autocorrelation of near-surface air temperature:

$$r(\tau) = \frac{\overline{T'(t)T'(t+\tau)}}{\overline{T'(t)^2}}. \quad (1)$$

Above, r is the autocorrelation, T is daily temperature, and τ is the time lag. An overline denotes a time average, and primes denote departures from the day-of-year time average, so that the seasonal cycle is removed. The day-of-year time average is computed on a per-model basis by averaging over all ensemble members for PAMIP experiments, and all years and ensemble members for CMIP6 output. This process is repeated separately for the pa-piArcSIC and pa-futArcSIC PAMIP experiments, and similarly for the pre-industrial and future time periods for CMIP6. As in Li and Thompson (2021), the global warming trend is removed from CMIP6 output prior to this, by subtracting a 10-year running mean reference timeseries, averaged over ensemble members, for each model.

Results are presented as percentage changes in the autocorrelation squared,

$$\Delta r_{\tau}^2 = \left(\frac{\overline{r_{\tau, \text{future}}^2}}{\overline{r_{\tau, \text{pre-industrial}}^2}} - 1 \right) \times 100, \quad (2)$$

which measures the change in variance explained by the lag- τ autocorrelation. Results are shown for $\tau = 5$ days in the main text, and $\tau = 10$ and 15 days in Supporting Information S1.

In order to evaluate the sensitivity of our results to the persistence metric used, we also include an analysis of changes in the length of warm and cold spells for the PAMIP and CMIP6 experiments (following Pfliederer & Coumou, 2018) in Supporting Information S1. We define warm days to be those where T' is greater than zero, and cold days to be those where T' is less than zero. Periods of consecutive warm days or cold days are then identified at each grid point, and the length of each warm or cold spell is saved. Changes in this metric are presented as changes in the average length of all warm and cold spells identified at a given grid point, between the pre-industrial and future time periods.

2.3. Idealized Model

To interpret the results we obtain from the PAMIP runs, we also analyze experiments run with an idealized GCM using the Isca modeling framework (Vallis et al., 2018). The model we use is similar to that described by Feldl and Merlis (2021). It is configured with a semi-gray radiative transfer scheme, with seasonally varying insolation. The representation of moist processes in the model is heavily simplified (Frierson, 2007; O'Gorman & Schneider, 2008), and clouds are omitted entirely. At the surface, the model is configured as an aquaplanet, comprised of a slab ocean with prescribed ocean heat transport (Merlis et al., 2013) and a simple representation of thermodynamic sea-ice (Feldl & Merlis, 2021; Zhang et al., 2022). A full description of the model is given in Supporting Information S1. The experiments run using Isca are described in Section 3.2.

2.4. Statistical Significance

Statistical significance is assessed by producing bootstrap confidence intervals for summary statistics of interest (e.g., Δr^2). This procedure constructs new ensembles from a random sampling of the individual members for each model (with replacement), treating model years as separate ensemble members for CMIP6 and Isca output. This process is repeated 1,000 times, and for each re-sampling the summary statistic is recomputed to produce a distribution from which confidence intervals are constructed. To compute bootstrap confidence intervals, we use the Python package ARCH (Sheppard, 2023) which uses a bias-corrected and accelerated bootstrap to adjust for the effects of bias and skewness on the bootstrap distribution (Efron & Tibshirani, 1994).

3. Results

3.1. Changes in Persistence

We begin by exploring changes in persistence for the four models that contributed pa-piArcSIC and pa-futArcSIC experiment runs to PAMIP. Figure 1a shows the multi-model mean percent change in the lag 5-day autocorrelation squared, $\Delta r_{\tau=5}^2$ (Equation 2), which quantifies the change in variance explained by persistence. For completeness, the response of the individual models is shown in Figure S1 in Supporting Information S1. For the PAMIP multi-model mean shown in Figure 1a, stippling is shown when at least 3 of the models exhibit a significant response at the 95% confidence level, and agree on the sign of the response. In general, persistence changes in the PAMIP experiments are weak or modest in magnitude (usually $\lesssim 50\%$). The strongest changes occur over the ocean, and are most prominent in the North Atlantic and low-Arctic, specifically within the

Changes in surface temperature persistence in PAMIP and CMIP experiments

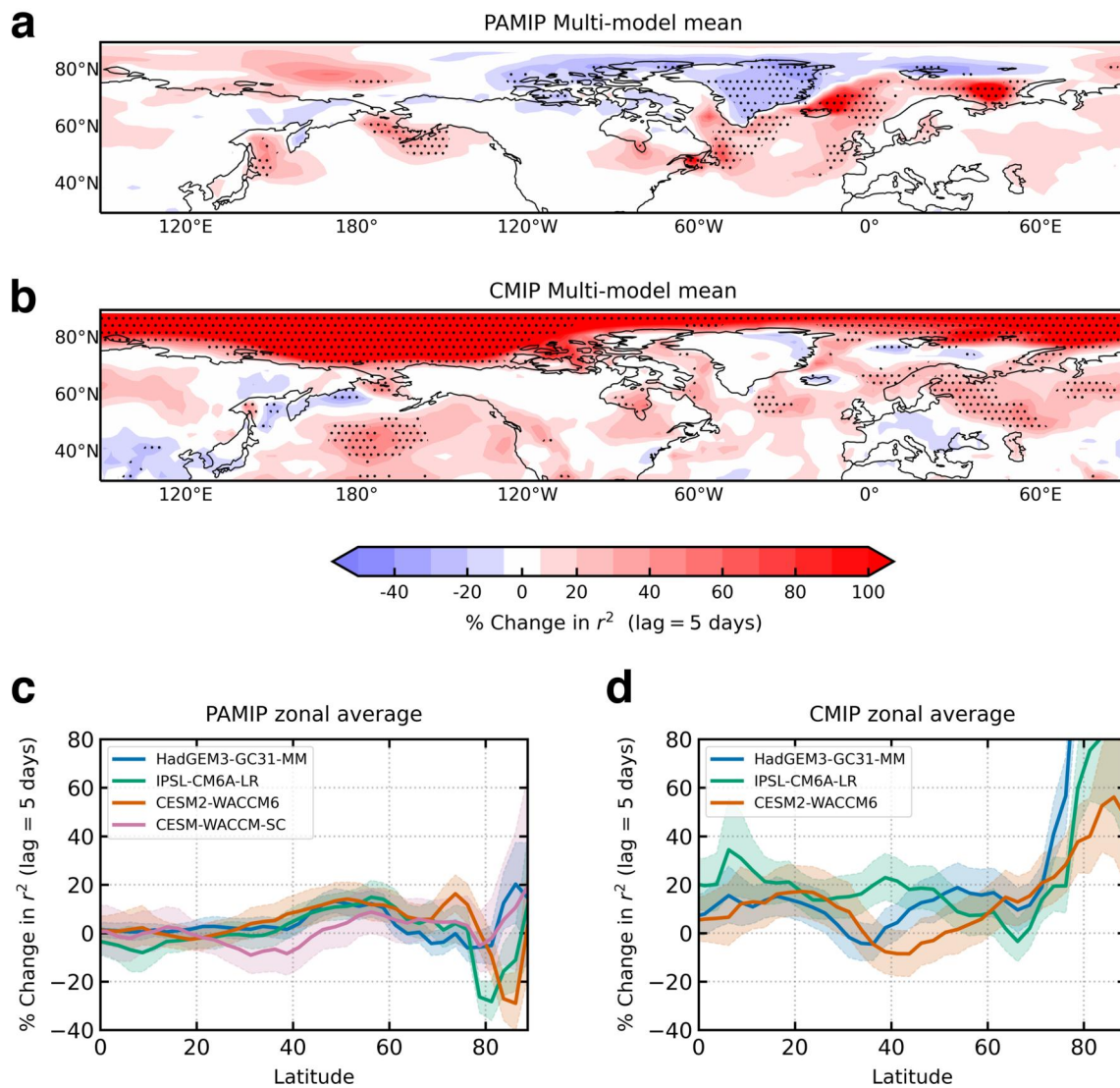


Figure 1. Changes in persistence in Polar Amplification Inter-model Comparison Project (PAMIP) and CMIP6 experiments. Contour plots show the percentage change in the lag 5-day autocorrelation squared, comparing pa-futArcSIC and pa-piArcSIC experiments for PAMIP (panel a), and 30 year pre-industrial and future periods for CMIP6 (panel b; see text for details). In each panel, the multi-model mean change in persistence is shown. For the PAMIP runs, stippling indicates that at least three of the four models return a significant response at the 95% level, and agree on the sign of the response. For the CMIP6 runs, stippling indicates the same criterion is met by two of the three models considered. The bottom two panels (c, d) show the zonally averaged response for each of the models considered. Shading shows 95% confidence intervals. In panel d, the persistence obtained with HadGEM3-GC31-MM in the Arctic ($\sim 300\%$) is much larger than that obtained by the other models, or in any model in midlatitudes. In order to improve readability, the y-axis in panel (d) is truncated. A version of this panel with an extended y-axis is included in Figure S5 in Supporting Information S1.

Norwegian and Barents seas. This is consistent with the circulation response to sea-ice loss being stronger over ocean compared with land (see, e.g., Figure 8 of Smith et al., 2022). Weaker increases in persistence can also be identified north of Siberia, and on the coasts of the Pacific Ocean. The zonal-mean persistence response for the individual PAMIP models is shown in Figure 1c, with shading showing 95% confidence intervals. In the zonal-mean, a significant increase in midlatitude persistence can be identified for three of the four models. The magnitude of this change is small ($\approx 15\%$), partially due to the absence of persistence changes over land.

In Figure 1, we only show results for lag $\tau = 5$ days. Equivalent analysis for $\tau = 10$ days and $\tau = 15$ days is shown in Figure S2 in Supporting Information S1. The spatial pattern of the lag-10 and lag-15 day persistence response in

each model is similar to that shown in Figure 1, but the magnitude of the response is larger (consistent with Li & Thompson, 2021). This is partially because changes in persistence are communicated as a percentage change, and the pre-industrial value of the autocorrelation squared is very small at longer time lags in the low-Arctic, where the largest changes occur (i.e., the denominator in the percentage change is smaller).

To compare the response of persistence to sea-ice loss with the total change induced by greenhouse gas emissions, the multi-model mean persistence change obtained from CMIP6 runs is shown in Figure 1b (restricted to the models analyzed for PAMIP). For each model, “pre-industrial” and “future” time periods are selected for each model so that the 30-year average sea-ice area is the same as that obtained in the corresponding PAMIP experiment. Stippling indicates a significant response at the 95% level when compared with inter-annual variability is obtained in at least two of the three models considered, and that these models agree on the sign of the response. The results obtained for the individual models are shown in Figure S3 in Supporting Information S1, and are qualitatively similar to those obtained by Li and Thompson (2021) (see their Extended Data Figure 3 for $\Delta r_{\tau=5}^2$ obtained from the NCAR CESM1 large ensemble).

The percent change in midlatitude and low-Arctic persistence in the PAMIP experiments is of a similar magnitude to that obtained in the CMIP6 runs, indicating that sea-ice loss may drive a significant amount of the total persistence change in these regions. However, persistence changes in the high-Arctic are strikingly different in the CMIP6 runs compared with PAMIP. For CMIP6, the large persistence increases occur in the high-Arctic for each model, whereas in the PAMIP output the persistence change in this region is far weaker, and the sign of the response varies between the models. Similar conclusions can be drawn by comparing the zonal-mean persistence responses for each model, shown on the bottom row of Figure 1 (a version of Figure 1d with an extended y-axis is included in Figure S5 in Supporting Information S1). Large persistence changes in the Arctic are to be expected under climate change, as melting sea-ice exposes open ocean which has a higher effective heat capacity, thus increasing its thermal inertia (Li & Thompson, 2021).

The unexpectedly weak response of high-Arctic persistence in the PAMIP simulations may be an artifact of the nudging methodology used by these experiments to remove sea-ice. This approach introduces an additional large, time-varying term into the surface energy budget in regions where the sea-ice loss is induced (e.g., England et al., 2022), and it is plausible that this may have unwanted side-effects on surface temperature variability. For example, the additional nudging term indirectly acts against the tendency of surface temperature (e.g., adding heat when the surface is “too cold” and undesired ice begins to form), which will have the effect of reducing the persistence of temperature anomalies.

In order to verify the robustness of our results to the choice of persistence metric, and to provide a link between changes in the autocorrelation and a more tangible feature of surface weather, we have also analyzed persistence changes in terms of the change in the average length of warm and cold spells (as defined in Section 2.2). The ensemble mean response in this metric obtained from the PAMIP and CMIP experiments is shown in Figure S4 in Supporting Information S1. In general terms, both methods reveal similar pattern of response. In Figure S4 in Supporting Information S1, persistence changes in PAMIP are found to be greatest over ocean, as in Figure 1a. For reference, the largest persistence increases in Figure 1a, found in the Norwegian and Barents seas (where $\Delta r_{\tau=5}^2 \approx 100\%$), correspond to an increase in the average length of warm and cold spells of roughly 0.5 days. When applied the CMIP6 runs, the results obtained using the two metrics differ more than for PAMIP. In particular, the weak increase in persistence over the North Atlantic indicated by the change in autocorrelation (in Figure 1b) is not replicated as a change in the average length of warm or cold spells. However, the large increase in Arctic persistence identified for CMIP6 remains, as does the absence of an increase in Arctic persistence in PAMIP. Using the new metric, the average length of warm and cold spells in the Arctic (zonally averaged) increases by approximately 2 days.

3.2. Interpretation With Idealized Models

Two routes through which sea-ice loss can affect surface temperature persistence are: (a) by altering the low-level equator-to-pole temperature contrast and inducing circulation changes (Cohen et al., 2019), and (b) by exposing open ocean, which increases the effective heat capacity of the surface (Li & Thompson, 2021). To interpret the persistence response in the PAMIP and CMIP6 experiments analyzed in Section 3.1, we consider results from an

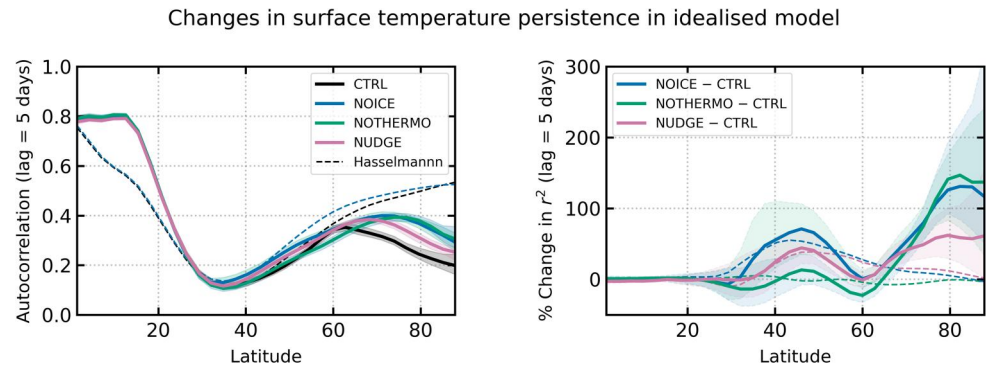


Figure 2. Response of surface temperature persistence to sea-ice loss in idealized GCM experiments. The left-hand panel shows the time- and zonal-mean lag 5-day temperature autocorrelation as a function of latitude. The right-hand panel shows the time- and zonal-mean percentage change in the lag 5-day autocorrelation squared, between experiments where some form of sea-ice loss is imposed (NOTHERMO, NOICE, NUDGE) and the control experiment (CTRL). In both panels, shading shows 95% confidence intervals. Output from the toy-model described by Equation 3 is shown as dashed curves. The GCM experiment from which the forcing, v_{10} , is obtained is indicated by colors, which correspond to those used for the full GCM output.

idealized GCM. The idealized model's simplicity (relative to a fully coupled AOGCM) allows us to configure a series of experiments designed to isolate routes (a) and (b) above.

We run four experiments: CTRL, NOTHERMO, NOICE, and NUDGE. The first, CTRL, is a control experiment where the model is run in its “full configuration,” with thermodynamic sea-ice included. In the second, NOTHERMO, the thermodynamic sea-ice code is switched off, and a seasonally varying ice-albedo, derived from the CTRL experiment, is prescribed in its place. In the third experiment, NOICE, the prescribed albedo from NOTHERMO is removed so that there is no representation of sea-ice in the model at all. Finally, the NUDGE experiment is run in the CTRL configuration, but with an additional term introduced to the thermodynamic sea-ice code which relaxes the sea-ice thickness toward zero on a timescale of 1 day, so that the equilibrated NUDGE simulation is ice-free. This methodology is designed to mimic that used in the PAMIP experiments. Further details describing the precise methodology used are given in Supporting Information S1.

Figure 2 shows the zonally-averaged autocorrelation (left panel), and persistence response (right panel) obtained in each experiment. The total effect of sea-ice loss on persistence can be assessed by comparing the experiments NOICE and CTRL (solid blue and black lines, respectively). This comparison shows that sea-ice loss has a local effect on persistence in the Arctic, which increases by $\approx 150\%$, as well as a remote effect on persistence in midlatitudes, which increases by $\approx 70\%$. The structure of the midlatitude persistence response in the idealized NOICE experiment is similar to the structure of the zonal mean response in PAMIP (shown in Figure 1), but the magnitude of the response is much greater in the idealized model. This is unsurprising, given that sea-ice is completely removed in the NOICE experiment, compared with only partial sea-ice loss in PAMIP. Additional differences in the persistence response obtained with the idealized NOICE experiment compared with PAMIP (e.g., the large persistence response in the Arctic in NOICE) may arise as an artifact of the nudging methodology used by the PAMIP AOGCMs to constrain sea-ice, and this possibility is explored later in this section.

In the NOTHERMO configuration (solid green lines in Figure 2), the idealized model's sea-ice code is replaced by a prescribed sea-ice albedo (obtained from the CTRL experiment). In this experiment, the response of the zonally- and annually-averaged temperature and circulation is negligible (Figures S6 and S7 in Supporting Information S1); therefore, the objective of comparing the experiments NOTHERMO and CTRL is to isolate route (b) above, namely the effect of sea-ice loss on persistence via an increased surface heat capacity. We note that while the annually-averaged temperature in these simulations is similar, they do exhibit seasonal differences (the increased surface heat capacity in NOTHERMO suppresses the seasonal cycle of surface temperature; cf. Feldl & Merlis, 2021). This will drive seasonal circulation changes, affecting the persistence response (see Figure S8 in Supporting Information S1, which shows the persistence response for NOTHERMO computed for winter and summer separately), but we believe that the impact of this effect on the annual mean response is small (see Figure S8 in Supporting Information S1, which additionally shows the persistence response *driven by circulation*

changes—quantified using a toy model for temperature variability, introduced below—is negligible in the annual mean). In Figure 2, the persistence increase in the Arctic in NOTHERMO is very similar to that induced by total sea-ice loss, suggesting that persistence increases in the Arctic are driven by sea-ice thermodynamic effects. By contrast, removing sea-ice thermodynamics from the model has little influence on persistence in midlatitudes (change consistent with zero), which is suggestive of a dynamical origin for the midlatitude persistence response in the NOICE experiment. The Arctic persistence increase obtained in the idealized NOTHERMO experiment is very similar to the high-latitude response in the CMIP6 output, which is absent in PAMIP (Figure 1).

When sea-ice is removed from the model by nudging the sea-ice thickness toward zero (NUDGE; solid pink lines in Figure 2), persistence changes are reduced relative to those obtained in the NOICE experiment, consistent with the suggestion in the previous section that the weak persistence response in PAMIP may be an artifact of the methodology used to constrain sea-ice. The idealized model results indicate that this effect may not be limited to the high-Arctic, as midlatitude persistence changes in the NUDGE experiment are also suppressed relative to the NOICE experiment. We note that in two of the PAMIP models, IPSL-CM6A-LR and CESM2-WACCM6, zonal-mean persistence (Figure 1d) actually decreases in the high Arctic (including over some ocean regions; Figure S1 in Supporting Information S1). This response is *consistent* with our hypothesis that nudging acts to reduce persistence in the ice-constrained climate, and could arise from a particularly strong “spurious effect” of the nudging methodology on the persistence response in these simulations. However, it is also possible that another process (e.g., changes in regional circulation) is acting to reduce persistence locally, and that this, in combination with the spurious effect of the sea-ice nudging, leads to the identified persistence decreases.

To further investigate the effect of changes in atmospheric circulation on persistence, we consider the following toy-model for temperature variability:

$$\frac{dT}{dt} = \lambda_f K v_{10}(t) - \lambda_d T, \quad (3)$$

similar to that described by Frankignoul and Hasselmann (1977). Above, T is the anomalous near-surface air temperature, and dT/dt is the local rate of change of temperature with respect to time. We assume that surface temperature variability is forced by anomalous near-surface (10 m) meridional wind, v_{10} . This is intended to represent advection by the meridional wind through a mean meridional temperature gradient (Schneider et al., 2015; Tamarin-Brodsky et al., 2020), as well as the subsequent indirect effect this has on turbulent heat fluxes (Frankignoul & Hasselmann, 1977). In the former interpretation, K represents a constant mean meridional temperature gradient, while in the latter interpretation, K is a constant of proportionality that relates the air-sea temperature difference to the near-surface meridional wind (as in Frankignoul & Hasselmann, 1977). $\tau_f = 1/\lambda_f$ is the forcing timescale. In Equation 3, the autocorrelation of temperature is independent of $\lambda_f K$ (which only affects the amplitude of the temperature anomalies), so we set $\lambda_f K = 1$ arbitrarily. Surface temperature variability generated by this forcing is then damped on a timescale $\tau_d = 1/\lambda_d$, associated with both turbulent and radiative processes. To use this model to interpret the GCM results, we integrate Equation 3 forwards in time using v_{10} output from each idealized GCM experiment. Each experiment uses the same value for λ_d , tuned so that the lag 5-day temperature autocorrelation (in midlatitudes), obtained using v_{10} from the CTRL simulation, roughly matches that obtained directly from the temperature output from the CTRL simulation (solid black line in Figure 2, left panel). This leads us to set $\lambda_d = 5 \times 10^{-6} \text{ s}^{-1}$, corresponding to a damping timescale of 2.3 days.

Changes in persistence obtained from the toy-model are shown in Figure 2 (right panel) as dashed lines. Applying v_{10} from the NOTHERMO experiment has no effect on the autocorrelation (relative to that obtained with v_{10} from the CTRL experiment; see the green dashed line). At high latitudes, this is consistent with the notion that persistence changes in the GCM simulation are due changes in the thermodynamic properties of the surface, which are not represented in the toy-model. When v_{10} from the NOICE and NUDGE experiments (shown with dashed blue and pink lines, respectively, in Figure 2) are used in the toy-model, the midlatitude persistence changes (relative to CTRL) are comparable in magnitude to those obtained in the full GCM simulations (compare the solid and dashed lines in Figure 2, right panel), consistent with persistence increases in midlatitudes having a dynamical origin. Specifically, the effect of v_{10} on temperature persistence in Equation 3 is due to changes in the frequency spectrum of v_{10} , with more persistent meridional wind anomalies causing an increase in surface temperature persistence.

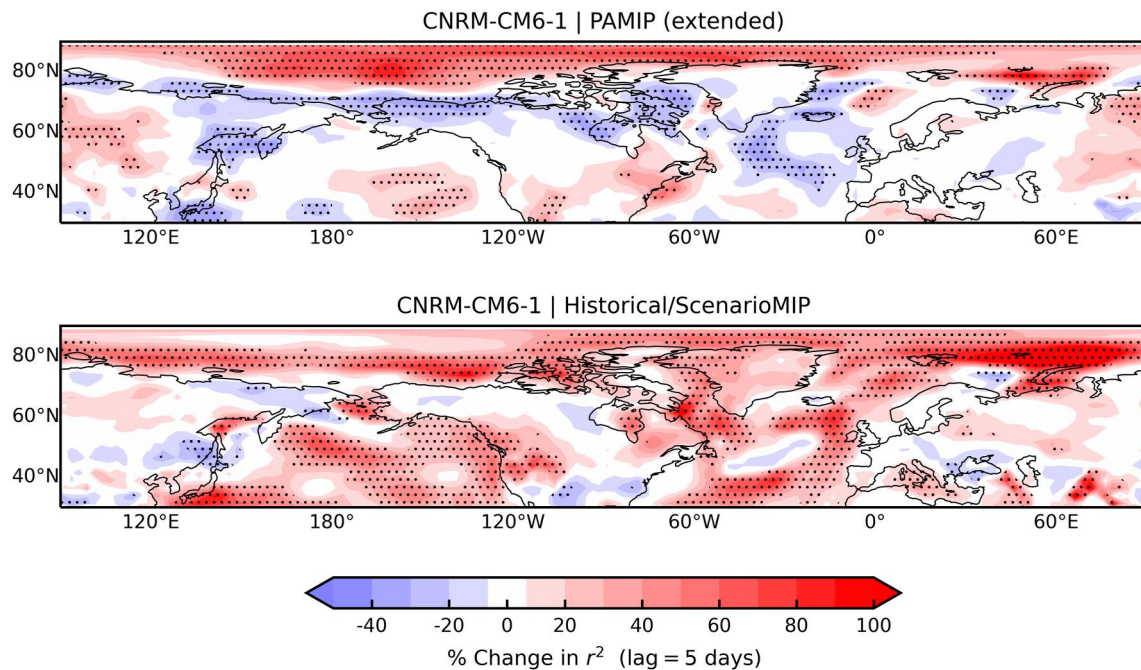


Figure 3. Comparison of persistence changes in CNRM-CM6-1 extended Polar Amplification Inter-model Comparison Project (PAMIP) runs (pa-futArcSIC-ext and pa-futArcSIC-ext) and CMIP6 runs (historical/spp585). Note that for the PAMIP data, the comparison is between future and present day, as opposed to pre-industrial (used for the PAMIP time-slice experiments analyzed in Section 3.1). Color contours show the time-mean percentage change in the lag 5-day autocorrelation squared between the future and present day periods. Black stippling indicates a statistically significant change at the 95% confidence level. For the CMIP6 data, change is measured between 30 year pre-industrial and present day periods, selected so that the time averaged sea-ice area is equal to that in the equivalent PAMIP run.

4. Discussion and Conclusions

We have investigated the effect of sea-ice loss on surface temperature persistence using results from PAMIP AOGCM simulations. Over ocean, sea-ice loss induces modest increases in surface temperature persistence in midlatitudes and the low-Arctic, whereas over land, persistence changes due to sea-ice loss are found to be weak. In regions where persistence increases in the PAMIP runs, the magnitude of change is similar to that obtained in CMIP6 simulations, suggesting that sea-ice loss may play an important role in shaping persistence changes under climate change (Li & Thompson, 2021). To interpret the results obtained from PAMIP, we ran additional simulations with forced sea-ice loss using an idealized GCM. Using these experiments, we suggest that midlatitude persistence increases due to sea-ice loss are mediated by changes in atmospheric circulation. More specifically, we infer that increased temperature persistence arises from an increase in the autocorrelation of the near-surface meridional wind. However, we have not identified the mechanisms through which changes in the near-surface wind are related to changes in the location and strength of the storm tracks, which have been shown to weaken in response to Arctic sea-ice loss (Hay et al., 2023; Kang et al., 2023; Shaw & Smith, 2022). Additionally, we note that processes missing from the idealized GCM, for example, ocean dynamics, and zonally asymmetric circulation features arising from topography and land-sea contrast, may also play a role in the persistence response obtained in PAMIP.

Our analysis of CMIP6 simulations, along with a similar analysis presented by Li and Thompson (2021), indicates that large persistence increases should also be expected for the high-Arctic under climate change. Simple arguments, based on sea-ice loss causing an increase in the effective heat capacity of the surface, suggest that such a change should be expected. Furthermore, this mechanism is found to operate in our idealized GCM simulations. However, the response of surface temperature persistence in the high-Arctic to sea-ice loss is found to be weak in PAMIP. We suggest that this may be an artifact of the nudging methodology used by the PAMIP experiments to constrain sea-ice, and we find that persistence changes are suppressed in an idealized GCM simulation where sea-ice loss is induced using nudging.

We would not expect the response of surface temperature persistence to be suppressed in experiments where sea-ice loss is induced via modification of the surface albedo, as this method does not introduce an additional term into

the surface energy budget. Support for this viewpoint is offered in Figure 3, which compares persistence changes due to sea-ice loss versus climate change using additional PAMIP and CMIP6 simulations, run using CNRM-CM6-1 (a different model to those analyzed thus far). For this model, persistence changes due to sea-ice loss are evaluated using two 100 year PAMIP runs forced with present day and future SICs constrained using albedo modification, denoted pa-pdArcSIC-ext and pa-futArcSIC-ext, respectively (Smith et al., 2019). In this comparison, high-Arctic persistence changes in the PAMIP and CMIP6 runs are comparable in magnitude, although we note that caution should be exercised when drawing conclusions from a single model. In addition to causing an increase in persistence, one would expect that an increase in the surface effective heat capacity would damp the amplitude of surface temperature variability; this suggestion is consistent with results presented by Blackport and Kushner (2016), who show that the standard deviation of 2 m temperature decreases over the Arctic in a coupled model (CCSM4) with sea-ice constrained by albedo modification. Ideally, a comparison of the effects of albedo modification versus nudging (and additionally the “ghost flux” approach described by Deser et al. (2015), which is qualitatively similar to nudging; England et al., 2022) would be made using the same model (i.e., similar to Sun et al., 2020), but unfortunately no runs with daily data were available for us to perform this analysis. Nonetheless, our results support the conclusion of England et al. (2022), that methods used to constrain sea-ice loss in coupled models may have spurious side-effects.

Data Availability Statement

All data required to reproduce the figures included in the main text and supporting information has been archived at: <https://doi.org/10.5281/zenodo.10009510> (Lewis et al., 2023).

Acknowledgments

NTL, WJMS, and JAS were supported by Natural Environment Research Council Grant ArctiCONNECT (NE/V005855/1). We are grateful to Yannick Peings for sharing the CESM-WACCM-SC PAMIP data, and to Yu-Chiao Liang for sharing the CESM2-WACCM6 PAMIP data. We would like to thank two anonymous reviewers, whose feedback aided us in improving the focus and clarity of the manuscript.

References

- Barnes, E. A., & Screen, J. A. (2015). The impact of arctic warming on the midlatitude jet-stream: Can it? Has it? Will it? *Wiley Interdisciplinary Reviews: Climate Change*, 6(3), 277–286. <https://doi.org/10.1002/wcc.337>
- Blackport, R., & Kushner, P. J. (2016). The transient and equilibrium climate response to rapid summertime sea ice loss in CCSM4. *Journal of Climate*, 29(2), 401–417. <https://doi.org/10.1175/JCLI-D-15-0284.1>
- Butler, A. H., Thompson, D. W. J., & Heikes, R. (2010). The steady-state atmospheric circulation response to climate change-like thermal forcings in a simple general circulation model. *Journal of Climate*, 23(13), 3474–3496. <https://doi.org/10.1175/2010JCLI3228.1>
- Cohen, J., Screen, J. A., Furtado, J. C., Barlow, M., Whittleston, D., Coumou, D., et al. (2014). Recent Arctic amplification and extreme mid-latitude weather. *Nature Geoscience*, 7(9), 627–637. <https://doi.org/10.1038/ngeo2234>
- Cohen, J., Zhang, X., Francis, J., Jung, T., Kwok, R., Overland, J., et al. (2019). Divergent consensus on Arctic amplification influence on midlatitude severe winter weather. *Nature Climate Change*, 10(1), 20–29. <https://doi.org/10.1038/s41558-019-0662-y>
- Deser, C., Lehner, F., Rodgers, K. B., Ault, T., Delworth, T. L., DiNezio, P. N., et al. (2020). Insights from Earth system model initial-condition large ensembles and future prospects. *Nature Climate Change*, 10(4), 277–286. <https://doi.org/10.1038/s41558-020-0731-2>
- Deser, C., Tomas, R. A., & Sun, L. (2015). The role of ocean-atmosphere coupling in the zonal-mean atmospheric response to Arctic sea ice loss. *Journal of Climate*, 28(6), 2168–2186. <https://doi.org/10.1175/JCLI-D-14-00325.1>
- Efron, B., & Tibshirani, R. J. (1994). An introduction to the bootstrap (1st ed.). <https://doi.org/10.1201/9780429246593>
- England, M. R., Eisenman, I., & Wagner, T. J. W. (2022). Spurious climate impacts in coupled sea ice loss simulations. *Journal of Climate*, 35(22), 3801–3811. <https://doi.org/10.1175/JCLI-D-21-0647.1>
- Feldl, N., & Merlis, T. M. (2021). Polar amplification in idealized climates: The role of ice, moisture, and seasons. *Geophysical Research Letters*, 48(17), e94130. <https://doi.org/10.1029/2021GL094130>
- Francis, J. A., & Vavrus, S. J. (2012). Evidence linking Arctic amplification to extreme weather in mid-latitudes. *Geophysical Research Letters*, 39(6), L06801. <https://doi.org/10.1029/2012GL051000>
- Frankignoul, C., & Hasselmann, K. (1977). Stochastic climate models. Part II Application to sea-surface temperature anomalies and thermocline variability. *Tellus*, 29(4), 289–305. <https://doi.org/10.3402/tellusa.v29i4.11362>
- Frierson, D. M. W. (2007). The dynamics of idealized convection schemes and their effect on the zonally averaged tropical circulation. *Journal of the Atmospheric Sciences*, 64(6), 1959–1976. <https://doi.org/10.1175/JAS3935.1>
- Hay, S., Priestley, M. D., Yu, H., Catto, J. L., & Screen, J. A. (2023). The effect of arctic sea-ice loss on extratropical cyclones. *Geophysical Research Letters*, 50(17), e2023GL102840. <https://doi.org/10.1029/2023GL102840>
- Kang, J. M., Shaw, T. A., & Sun, L. (2023). Arctic Sea ice loss weakens northern Hemisphere summertime Storminess but not until the late 21st century. *Geophysical Research Letters*, 50(9), e2022GL102301. <https://doi.org/10.1029/2022GL102301>
- Lewis, N. T., Seviour, W. J. M., Roberts-Straw, H. E., & Screen, J. A. (2023). Data supporting ‘the response of midlatitude surface temperature persistence to Arctic Sea-Ice loss’ by Neil T Lewis, William J M Seviour, Hannah E Roberts-Straw, and James A Screen [Dataset]. Zenodo. <https://doi.org/10.5281/zenodo.10009510>
- Li, J., & Thompson, D. W. J. (2021). Widespread changes in surface temperature persistence under climate change. *Nature*, 599(7885), 425–430. <https://doi.org/10.1038/s41586-021-03943-z>
- Merlis, T. M., Schneider, T., Bordoni, S., & Eisenman, I. (2013). Hadley circulation response to orbital precession. Part II: Subtropical continent. *Journal of Climate*, 26(3), 754–771. <https://doi.org/10.1175/JCLI-D-12-00149.1>
- Notz, D., & Stroeve, J. (2016). Observed Arctic sea-ice loss directly follows anthropogenic CO₂ emission. *Science*, 354(6313), 747–750. <https://doi.org/10.1126/science.aag2345>
- O’Gorman, P. A., & Schneider, T. (2008). The hydrological cycle over a wide range of climates simulated with an idealized GCM. *Journal of Climate*, 21(15), 3815–3832. <https://doi.org/10.1175/2007JCLI2065.1>

- Pfleiderer, P., & Coumou, D. (2018). Quantification of temperature persistence over the Northern Hemisphere land-area. *Climate Dynamics*, 51(1–2), 627–637. <https://doi.org/10.1007/s00382-017-3945-x>
- Schneider, T., Bischoff, T., & Plotka, H. (2015). Physics of changes in synoptic midlatitude temperature variability. *Journal of Climate*, 28(6), 2312–2331. <https://doi.org/10.1175/JCLI-D-14-00632.1>
- Screen, J. A., & Blackport, R. (2019). How robust is the atmospheric response to projected Arctic Sea ice loss across climate models? *Geophysical Research Letters*, 46(20), 11406–11415. <https://doi.org/10.1029/2019GL084936>
- Screen, J. A., & Simmonds, I. (2010). The central role of diminishing sea ice in recent Arctic temperature amplification. *Nature*, 464(7293), 1334–1337. <https://doi.org/10.1038/nature09051>
- Shaw, T. A., & Smith, Z. (2022). The midlatitude response to polar sea ice loss: Idealized slab-ocean aquaplanet experiments with thermodynamic sea ice. *Journal of Climate*, 35(8), 2633–2649. <https://doi.org/10.1175/JCLI-D-21-0508.1>
- Sheppard, K. (2023). bashtage/arch version 5.5. *Zenodo*. <https://doi.org/10.5281/zenodo.7863349>
- Smith, D. M., Eade, R., Andrews, M. B., Ayres, H., Clark, A., Chripko, S., et al. (2022). Robust but weak winter atmospheric circulation response to future Arctic sea ice loss. *Nature Communications*, 13(1), 727. <https://doi.org/10.1038/s41467-022-28283-y>
- Smith, D. M., Screen, J. A., Deser, C., Cohen, J., Fyfe, J. C., García-Serrano, J., et al. (2019). The polar amplification model intercomparison project (PAMIP) contribution to CMIP6: Investigating the causes and consequences of polar amplification. *Geoscientific Model Development*, 12(3), 1139–1164. <https://doi.org/10.5194/gmd-12-1139-2019>
- Sun, L., Alexander, M., & Deser, C. (2018). Evolution of the global coupled climate response to Arctic sea ice loss during 1990–2090 and its contribution to climate change. *Journal of Climate*, 31(19), 7823–7843. <https://doi.org/10.1175/JCLI-D-18-0134.1>
- Sun, L., Deser, C., Tomas, R. A., & Alexander, M. (2020). Global coupled climate response to polar sea ice loss: Evaluating the effectiveness of different ice-constraining approaches. *Geophysical Research Letters*, 47(3), e85788. <https://doi.org/10.1029/2019GL085788>
- Tamarin-Brodsky, T., Hodges, K., Hoskins, B. J., & Shepherd, T. G. (2020). Changes in Northern Hemisphere temperature variability shaped by regional warming patterns. *Nature Geoscience*, 13(6), 414–421. <https://doi.org/10.1038/s41561-020-0576-3>
- Vallis, G. K., Colyer, G., Geen, R., Gerber, E., Jucker, M., Maher, P., et al. (2018). Isca, v1.0: A framework for the global modelling of the atmospheres of Earth and other planets at varying levels of complexity. *Geoscientific Model Development*, 11(3), 843–859. <https://doi.org/10.5194/gmd-11-843-2018>
- Zhang, X., Schneider, T., Shen, Z., Pressel, K. G., & Eisenman, I. (2022). Seasonal cycle of idealized polar clouds: Large eddy simulations driven by a GCM. *Journal of Advances in Modeling Earth Systems*, 14(1), e2021MS002671. <https://doi.org/10.1029/2021MS002671>